

Spectroscopy and photophysics of trimethyl-substituted derivatives of 5-deazaalloxazine. Experimental and theoretical approaches



Dorota Prukała^{a,*}, Mateusz Gierszewski^a, Maciej Kubicki^a, Tomasz Pędziński^a, Ewa Sikorska^b, Marek Sikorski^a

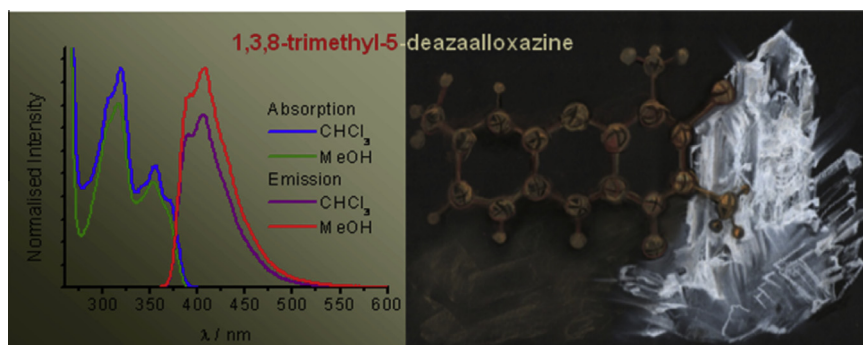
^a Faculty of Chemistry, Adam Mickiewicz University in Poznań, Umultowska 89B, 61-614 Poznań, Poland

^b Faculty of Commodity Science, Poznań University of Economics, al. Niepodległości 10, 61-875 Poznań, Poland

HIGHLIGHTS

- Photophysical properties of newly synthesized 5-deazaalloxazines were presented.
- Fluorescence lifetime measurements were performed in different solvents.
- The crystal structures of investigated compounds were determined by X-ray analysis.
- $S_0 \rightarrow S_1$, $S_0 \rightarrow T_1$ and $T_1 \rightarrow T_1$ transitions were calculated, using the TD-DFT methods.
- Electronic structures of 5-deazaalloxazines were calculated by the same methods.

GRAPHICAL ABSTRACT



ARTICLE INFO

Article history:

Received 4 May 2014

Received in revised form 6 September 2014

Accepted 11 September 2014

Available online 21 September 2014

Keywords:

Alloxazines
5-Deazaalloxazines
DFT study
Photophysics
UV–Vis spectroscopy
X-ray crystallography

ABSTRACT

Photophysical and structural properties of 5-deazaalloxazine derivatives were studied, with methyl substituent at the position 8 or 9 of the benzene ring and at the N(1) and N(3) positions. Crystal structures of the compounds were determined by X-ray diffraction method.

Electronic structure and $S_0 \rightarrow S_1$, $S_0 \rightarrow T_1$ and $T_1 \rightarrow T_1$ transition energies and oscillator strengths were calculated for 1,3,8- and 1,3,9-trimethyl-5-deazaalloxazine, using the TD-DFT methods. The calculations suggest that for 5-deazaalloxazine derivatives the lowest-lying singlet excited states have pure π, π^* nature. This is in contrast to the alloxazine derivatives, where two lowest-lying transitions are of π, π^* and n, π^* character, being isoenergetic in most cases. The theoretical data are compared to the experimental results, involving steady-state and time-resolved spectra. 1,3,8-Trimethyl-5-deazaalloxazine and 1,3,9-trimethyl-5-deazaalloxazine have longer fluorescence lifetimes and higher values of fluorescence quantum yield compared to the alloxazine derivatives in the same solvents, whereas the absorption maxima and emission maxima of studied compounds are blue-shifted as compared to trimethyl derivatives of alloxazine.

© 2014 Elsevier B.V. All rights reserved.

Introduction

5-Deazaflavin (with tricyclic 5-deazaalloxazine ring) occurs as a natural cofactor in yellow chromophores [1] in various bacteria and has been extensively used as an artificial coenzyme in

mechanistic studies with numerous flavoproteins [2]. For the past three decades, 5-deazaflavins (pyrimido[4,5-*b*]quinolin-2,4(3*H*,10*H*)-diones), where N-5 of the flavin is replaced by $-\text{CH}$, have received much attention, because of the discovery that they serve as cofactors for several flavin-dependent enzymatic reactions [3]. 5-Deazaflavins are potential riboflavin antagonists with their own redox system, different from that of riboflavin [3]. 5-Deazaalloxazines (pyrimido[4,5-*b*]quinoline-2,4(1*H*,3*H*)-diones) are ana-

* Corresponding author. Tel.: +48 61 8291593; fax: +48 61 8291555.

E-mail address: dprukala@amu.edu.pl (D. Prukała).

logs of 5-deazaflavins, they are also analogs of alloxazines (benzo[g]pteridine-2,4(1*H*, 3*H*)-diones).

Fig. 1 presents the structures of investigated compounds with structures of 5-deazaflavin and alloxazine for comparison.

It is postulated that alloxazines and 5-deazaalloxazines, for example lumichrome (7,8-dimethylalloxazine) and 5-deazaalumichrome (7,8-dimethyl-5-deazaalloxazine) have similar properties in their ground and excited singlet state, namely solvatochromism, ground and excited state pK_a , and small differences between their ground and excited state dipole moments [4]. Additionally, the common structure of 5-deazaflavin and 5-deazaalloxazine is that both contain the pyrimido[4,5-*b*]quinoline moiety and this type of compound is of importance owing to its various biological activities, especially antimalarial, antibacterial, analgesic and antitumor activities [3,5–9], which have led to its use in industrial drugs [10–12,5]. Different derivatives of 5-deazaalloxazine are also considered as suicide substrates for adenosine deaminase and inosine 5-monophosphate dehydrogenase [13].

Recently, there is growing interest in development of fluorescent nucleosides based on 5-deazaalloxazine that maintain the hydrogen-bonding properties of natural nucleoside bases [14,15]. To our surprise, although derivatives of 5-deazaalloxazine are of great interest in many aspects, there is only few literature data regarding their photophysical properties [16–18]. So the aim of the present work is to characterize spectroscopic and photophysical properties of 1,3,8-trimethyl-5-deazaalloxazine (138Me-5DAII) and 1,3,9-trimethyl-5-deazaalloxazine (139Me-5DAII). The experimental data are compared with theoretical studies by using time-dependent density functional theory (TD-DFT). Accordingly to our recent results [18], 5-deazaalloxazines show high values of fluorescence quantum yields, and show longer fluorescence lifetimes than their alloxazine analogues [19–23]. In addition, the data from theoretical calculations indicated that the lowest-energy transitions of 5-deazaalloxazines have pure π,π^* character, as in the case for derivatives of alloxazine the lowest π,π^* transition is accompanied by closely-located n,π^* transition [19–24]. 138Me-5DAII and 139Me-5DAII were synthesized using a method described by Yoneda et al. [25,26] in a two-step synthesis. We also present the detailed crystal structures of the investigated compounds.

Experimental

Materials

Solvents: methanol (MeOH), ethanol (EtOH), 2-propanol (2-PrOH), acetonitrile (ACN), chloroform (CHCl₃), methylene chloride (CH₂Cl₂), 1,4-dioxane (Diox), were of spectroscopic or HPLC grade (Aldrich, Merck). They were dried before use with 3 Å or 4 Å molecular sieves from Fluka.

*General procedure for the preparation of pyrimido[4,5-*b*]quinoline-2,4(1*H*,3*H*)-diones Step 1* [27]. To a stirred solution of *o*-methylaniline (or *m*-methylaniline) (3 ml) was added hydrochloric acid (36%, 6 mmol) and 1,3-dimethyl-6-aminouracil (6 mmol). The mixture was heated at 170–180 °C for 4–5 h. Diethyl ether was added after cooling and precipitated solids were collected by filtration. The corresponding 6-anilinouracils were obtained in 40–98% yields.

Step 2. The appropriate 6-anilinouracil derivative (1 g) was mixed with DMF (2 ml) and heated to 40 °C under stirring. Then phosphorus oxychloride (2.5 ml) was dropped into the mixture. The mixture was then heated at 80 °C for 0.5 h. After cooling, excess DMF and POCl₃ were evaporated *in vacuo*. The solids were diluted with 5% NH₄OH and then collected by suction filtration and washed with water. Crude products were recrystallized from glacial acetic acid. Obtained crystals were suitable for X-ray analysis.

Purity of all of the compounds studied was checked by thin layer chromatography and elemental analysis.

*1,3,8-Trimethylpyrimido[4,5-*b*]quinoline-2,4(1*H*,3*H*)-dione, (138Me-5DAII)* (isolated yield 55%; m.p. 230 °C); ¹H NMR (TFA-*d*): δ ppm: 2.79 (s, 3H, H₃C-C₈); 4.10 (s, 3H, H₃C-N₁); 3.71 (s, 3H, H₃C-N₃); 7.88 (d, 1H, H-7); 8.16 (s, 1H, H-9); 8.29 (d, 1H, H-6); **9.77** (s, 1H, H-C₅); Anal. Calcd for C₁₄H₁₃N₃O₂: C, 65.88; H, 5.10; N, 16.47. Found: C, 66.01; H, 4.99; N, 16.38.

*1,3,9-Trimethylpyrimido[4,5-*b*]quinoline-2,4(1*H*,3*H*)-dione, (139Me-5DAII)* (isolated yield (54%; m.p. 214 °C); ¹H NMR (TFA-*d*): δ ppm: 2.94 (s, 3H, H₃C-C₉); 4.16 (s, 3H, H₃C-N₁); 3.71 (s, 3H, H₃C-N₃); 7.98 (t, 1H, H-7); 8.23 (d, 1H, H-8); 8.30 (d, 1H, H-6); **9.87** (s, 1H, C-5); Anal. Calcd for C₁₄H₁₃N₃O₂: C, 65.88; H, 5.10; N, 16.47. Found: C, 65.92; H, 5.01; N, 16.40.

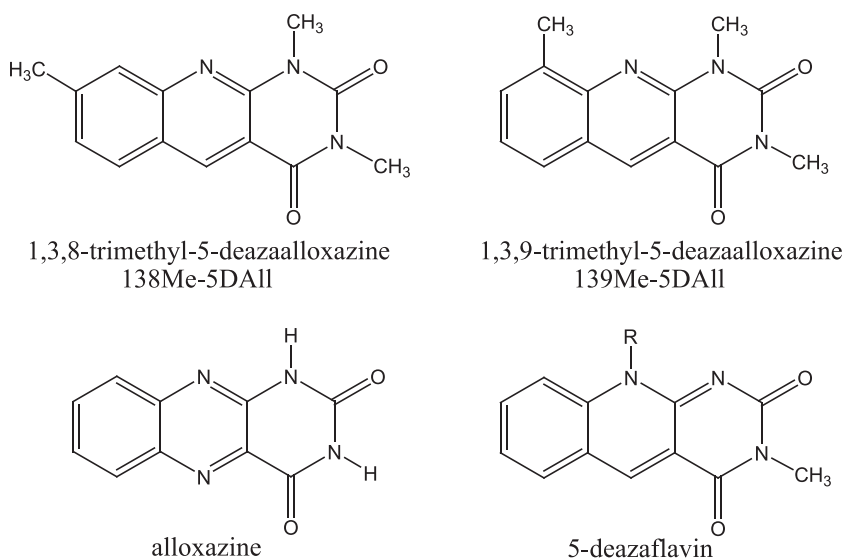


Fig. 1. Structures of 1,3,8-trimethyl-5-deazaalloxazine (138Me-5DAII) and 1,3,9-trimethyl-5-deazaalloxazine (139Me-5DAII), and their analogues: 5-deazaflavin and alloxazine.

Methods

UV/Vis measurements

All solutions were prepared on the same day as their absorbance, steady-state fluorescence, fluorescence excitation spectra were recorded and time-resolved fluorescence measurements performed. As the maximum of absorption, λ_{max} , for the lowest-energy transitions did not vary much between solvents, it was determined with three replicates at a reduced scanning rate. The same precautions were taken for the emission λ_{max} , the latter was also determined for several λ_{exc} values.

UV–Vis absorption spectra were recorded on JASCO V-650 spectrophotometer and on a Jobin Yvon-Spex Fluorolog 3-22 spectrofluorometer, using the option to measure absorption spectra; steady-state fluorescence excitation and emission spectra were also recorded on the same spectrofluorometer.

Fluorescence quantum yield were calculated relative to lumichrome as standard ($\Phi_{\text{F}} = 0.028$ in acetonitrile [20]). We used the method described by Horiba Jobin–Yvon (gradient method), with simultaneous measurements of absorption and fluorescence on the same machine (www.jyhoriba.co.uk). Maximum absorption of all solutions was kept below 0.1. The estimated absolute uncertainty of the calculated fluorescence quantum yield in 20 %.

Life-time measurements

All fluorescence lifetime measurements were performed using a time-correlated single-photon counting (TCSPC) method. Decays were measured with an IBH Consultants (Glasgow, Scotland) System 5000 fluorescence lifetime spectrometer equipped with a NanoLED diode ($\lambda_{\text{exc}} = 374$ nm, fwhm ≈ 800 ps) and with a Pico-Quant (Berlin, Germany) FluoTime 300 spectrometer with a 377 nm pulsed LED, fwhm ≈ 500 ps) as an excitation source. Both instruments are capable of measuring fluorescence lifetimes of 400 ps or shorter. Deconvolution of the fluorescence decay curves was performed using Version 4 of the IBH Consultants software (for 374 nm excitation) or FluoFit Fluorescence Decay Data Analysis Software (version 4.55) from PicoQuant (for 377 nm excitation).

^1H NMR measurements

^1H NMR spectra for 138Me-5DAII and 139Me-5DAII were recorded in TFA-d, as their solubility in typically used DMSO- d_6 was insufficient. The ^1H NMR spectra were recorded on a Varian Gemini 300 (300 MHz) Spectrometer. The internal standard was TMS. ^1H NMR spectra of compounds studied were analyzed by comparison to spectra calculated using the ACD/H NMR predictor [28].

X-ray diffraction analysis

Diffraction data for 138Me-5DAII and for 139Me-5DAII were collected at 100 K on an Agilent Technologies XCALIBUR diffractometer with EOS CCD detector using graphite-monochromated Mo K α radiation ($\lambda = 0.71073$ Å). The data were collected using the ω -scan technique to a maximum 2θ value of 60° and corrected for Lorentz and polarization effects [29]. Accurate unit-cell parameters were determined by a least-squares fit of 1440 (138Me-5DAII), and 14,443 (139Me-5DAII) reflections of the highest intensity, chosen from the whole experiment. The calculations were mainly performed within the WinGX program system [30]. The structure was solved by direct methods with SIR92 [31] refined by the full matrix least-squares method with SHELXL97. Non-hydrogen atoms were refined anisotropically. The hydrogen atoms from methyl groups were placed geometrically in idealized positions, and refined as rigid groups with their U_{iso} 's as 1.5 times U_{eq} of the appropriate carrier atom; all other hydrogen atoms were found in subsequent difference Fourier maps and isotropically refined.

Crystallographic data (excluding the structure factors) for the structural analysis have been deposited with the Cambridge Crystallographic Data Centre, Nos. CCDC-770192 (138Me-5DAII), and CCDC-770191 (139Me-5DAII). Copies of this information may be obtained free of charge from: The Director, CCDC, 12 Union Road, Cambridge, CB2 1EZ, UK. Fax: +44(1223)336 033, e-mail: deposit@ccdc.cam.ac.uk, or www: www.ccdc.cam.ac.uk.

TD-DFT calculations

Theoretical calculations have been studied by means of time-dependent density-functional theory (TD-DFT). The TD-DFT calculations were calculated using the B3LYP hybrid method [32] in conjunction with a modest 6-31 + g(d) split-valence polarized basis set [33]. Excitation energies and transition intensities were calculated for the optimized ground-state geometries. Oscillator strengths were determined in the dipole length representation. Calculations were performed using the GAUSSIAN 09 package of *ab initio* programs [34].

Results and discussion

Steady-state spectra of 138Me-5DAII and 139Me-5DAII

Absorption properties

Absorption spectra of 138Me-5DAII and 139Me-5DAII in selected organic solvents are presented in Fig. 2A and B. Table 1 summarizes absorption parameters for 138Me-5DAII and 139Me-5DAII. The compounds have two absorption maxima in the lowest-energy part of the spectrum (λ_1 and λ_2), usually well separated and with some structure, corresponding to two independent π, π^* transitions.

As we can see in Fig. 2A and B and Table 1, the two lowest-energy absorption maxima for 138Me-5DAII and 139Me-5DAII are located about 360 nm (λ_1) and about 315 nm (λ_2), and their exact positions practically are not dependent on solvent. The position of maximum of the lowest-energy band (λ_1) depends on the location of the methyl substituent on the benzene ring. Comparing the spectral properties of investigated compounds with those of 8-methyl-5-deazaalloxazine and 9-methyl-5-deazaalloxazine (which are unsubstituted on nitrogen atoms) [18], we note a small shift in the positions of the band maxima, and a change in the band shapes of the absorption spectra. In aprotic solvents, the λ_1 maxima of the lowest-energy bands in 8-methyl- and 9-methyl-5-deazaalloxazine are shifted hypsochromically comparing to the corresponding maxima of 138Me-5DAII and 139Me-5DAII, by about 6 nm.

Additionally, location of the two absorption maxima of 138Me-5DAII and 139Me-5DAII, are generally hypsochromically shifted, as compared to their "aza" analogues, namely 8-methyl- and 9-methylalloxazines [24]. The lowest-energy absorption bands of 5-deazaalloxazines, where the N(5) atom in the alloxazine ring is replaced by the C atom, have a more pronounced vibrational structure than the respective alloxazine absorption bands.

Emission properties

In Fig. 2C and D, we show the emission spectra of 138Me-5DAII and 139Me-5DAII in different organic solvents. Table 2 presents the emission parameters including the emission maxima, the fluorescence quantum yields, the fluorescence lifetime, the radiative rate constants, and the sum of the non-radiative rate constants of 138Me-5DAII and 139Me-5DAII. The absorption and the corrected fluorescence excitation spectra of all of the compounds agree well with each other.

Typical emission spectra of investigated compounds show a single bands of Gaussian shape. The emission maxima appear at about 420 nm (for 139Me-5DAII). But emission bands for 138Me-5DAII

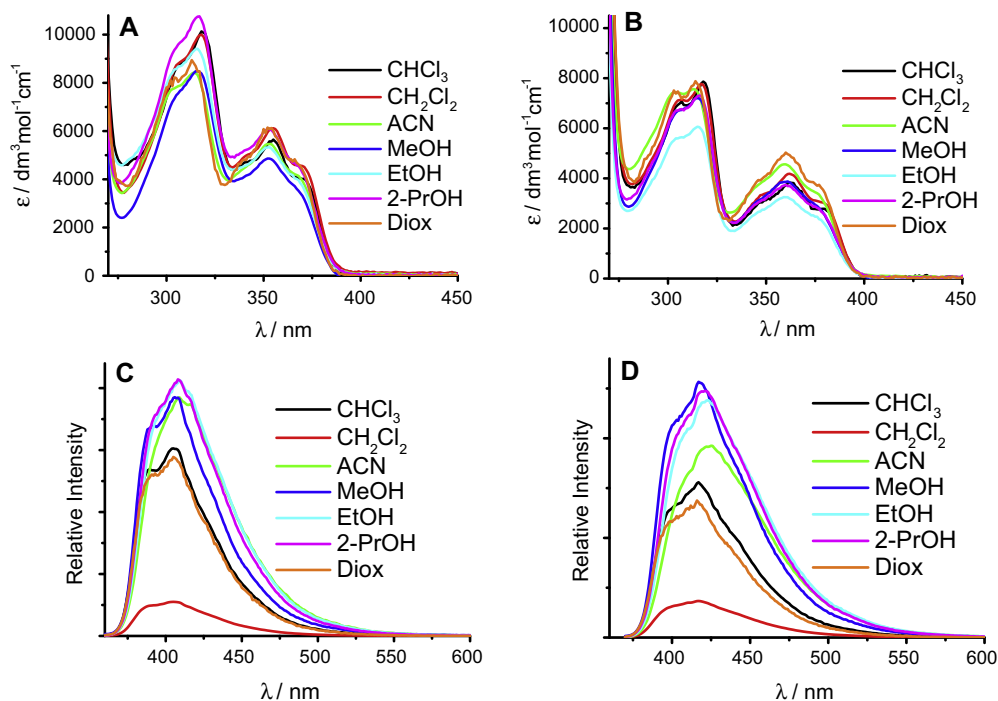


Fig. 2. A – Absorption spectra of 138Me-5DAll, B – absorption spectra of 139Me-5DAll, C – emission spectra ($\lambda_{\text{exc}} = 350$ nm) of 138Me-5DAll, D – emission spectra ($\lambda_{\text{exc}} = 360$ nm) of 139Me-5DAll, in selected organic solvents.

Table 1
Absorption parameters λ_i/nm for 138Me-5DAll and 139Me-5DAll.

Solvent	λ_1/nm^a	λ_2/nm^a
<i>138Me-5DAll</i>		
CHCl ₃	355	318
CH ₂ Cl ₂	355	318
ACN	353	314
2-PrOH	353	317
EtOH	353	316
MeOH	352	316
<i>139Me-5DAll</i>		
CHCl ₃	362	318
CH ₂ Cl ₂	362	317
ACN	359	313
2-PrOH	360	316
EtOH	359	315
MeOH	361	315

^a λ_1 , λ_2 are the positions of the two lowest-energy bands in the absorption spectra.

are blue-shifted if compared to the emission bands of 139Me-5DAll in the same solvents. The emission maxima of 138Me-5DAll are located at about 407 nm. The solvent polarity affects the exact position of the emission maxima; however this effect is rather small, particularly for 138Me-5DAll. There is a red shift of emission maxima in polar solvents (alcohols) as compared to apolar and aprotic solvents for both compounds. Interestingly, the substitution of the N(1) and N(3) by methyl groups does not change this tendency, thus the emission maxima for the compounds 138Me-5DAll and 139Me-5DAll are almost the same as those for their unsubstituted analogues: 8-methyl-5-deazaalloxazine and 9-methyl-5-deazaalloxazine [18]. Generally, the fluorescence emission maxima of alloxazines are red shifted as compared to those of their 5-deazaalloxazine analogues in the same solvents, as obvious from the data in literature [24].

Table 2
Photophysical data for the singlet states for 138Me-5DAll and 139Me-5DAll.

Solvent	λ_F/nm^a	Φ_F^a	τ_F/ns^a	$k_r/10^8 \text{ s}^{-1a}$	$\Sigma k_{nr}/10^8 \text{ s}^{-1a}$
<i>138Me-5DAll</i>					
CHCl ₃	406	0.11	2.21	0.50	4.01
CH ₂ Cl ₂	405	0.02	2.01	0.09	4.88
ACN	405	0.14	2.45	0.57	3.51
2-PrOH	408	0.15	2.96	0.51	2.87
EtOH	409	0.15	3.03	0.49	2.81
MeOH	409	0.14	2.82	0.50	3.05
<i>139Me-5DAll</i>					
CHCl ₃	417	0.17	3.92	0.43	2.11
CH ₂ Cl ₂	417	0.04	3.87	0.10	2.48
ACN	417	0.21	4.51	0.47	1.75
2-PrOH	421	0.27	6.89	0.39	1.06
EtOH	423	0.26	7.27	0.36	1.02
MeOH	425	0.28	7.90	0.35	0.91

^a λ_F the fluorescence emission maximum, Φ_F the fluorescence quantum yield, τ_F the fluorescence lifetime, k_r the radiative rate constant and Σk_{nr} the sum of non-radiative rate constants.

Photophysics of 138Me-5DAll and 139Me-5DAll

The fluorescence quantum yields, the lifetimes, the radiative and sum of the non-radiative decay constants for the lowest excited singlet state of 138Me-5DAll and 139Me-5DAll are presented in Table 2. The radiative and non-radiative decay constants were calculated as presented below:

$$k_r = \Phi_F/\tau_F, \quad \Sigma k_{nr} = (1 - \Phi_F)/\tau_F.$$

In all cases the fluorescence decays are well modelled by single exponential functions, as shown by the usual statistical criteria of “goodness-of-fit”.

Generally, the fluorescence quantum yields are high, the exact values, depending on solvent and compound, and are between 0.02 and 0.27. The higher values of fluorescence quantum yield

were noted in protic solvents (alcohols) compared to other solvents for the same derivative. 138Me-5DAll shows lower values of fluorescence quantum yield if comparing those of 139Me-5DAll at the same conditions. The quantum yields of 138Me-5DAll and 139Me-5DAll are about ten-fold higher as reported for their alloxazine analogues (8-methyl-5-deazaalloxazine and 9-methyl-5-deazaalloxazine) [18] in the same solvents. The fluorescence lifetimes (τ_F) of 138Me-5DAll are shorter than those of 139Me-5DAll and additionally are longer than for their “aza” analogues. This shows that the location of the methyl group on the alloxazinic skeleton affects the fluorescence lifetime (see Table 2 for details). Both of the investigated 5-deazaalloxazines have longer fluorescence lifetimes in alcohols than those in aprotic solvents. The radiative and non-radiative decay constants for both 5-deazaalloxazine derivatives (Table 2) show that the decay of their singlet state is dominated by the rates of non-radiative processes and are about two-ten-fold higher than the radiative constants.

Crystal structures

X-ray diffraction analysis shows that crystals of 138Me-5DAll ($0.4 \times 0.4 \times 0.1$ mm) and 139Me-5DAll ($0.3 \times 0.2 \times 0.15$ mm) have similar structures. The molecules of both compounds are almost planar and are connected by approximately linear hydrogen bonds in the crystals. Crystal structure and structure refinement parameters of 138Me-5DAll and 139Me-5DAll are given in Table 3. Fig. 3 presents an ORTEP drawing of 138Me-5DAll and 139Me-5DAll with the numbering scheme of the individual atoms, used also in the next part of the paper.

The molecules of 138Me-5DAll and 139Me-5DAll are arranged into molecular tapes, with the molecules in these tapes connected by the relatively strong intermolecular C–H...O hydrogen bonds, forming oligomers. The C6–H6...O4 and C5–H5...O4 hydrogen bonds in both 138Me-5DAll and 139Me-5DAll connect molecules into centrosymmetric dimmers. These dimmers are further connected to other dimmers and make infinite tapes by means of

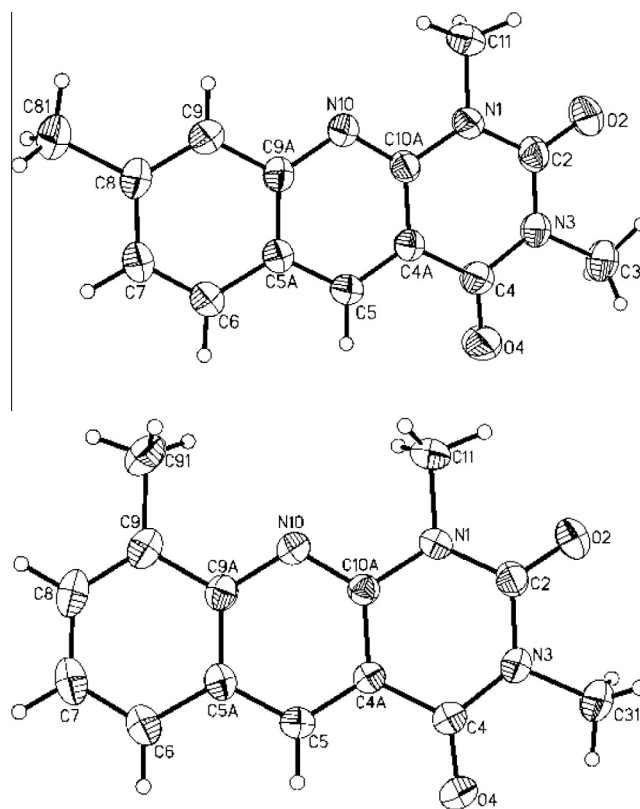


Fig. 3. Anisotropic-ellipsoid representation of 138Me-5DAll (top) and 139Me-5DAll (bottom), together with the numbering scheme. The ellipsoids are drawn at the 50% probability level; hydrogen atoms are represented by spheres of arbitrary radii.

C7–H7...O2 bonds. The hydrogen-bonded molecular tapes in the crystal structure of 138Me-5DAll and 139Me-5DAll are shown in Fig. 4. The tapes of molecules are stacked one onto another with an interplanar distance of ca. 3.4 Å.

The data on the hydrogen bonds are shown in Table 4.

Table 3

Crystal structures and structure refinement parameters for 138Me-5DAll and 139Me-5DAll.

Compounds	138Me-5DAll	139Me-5DAll
Chemical formula	C ₁₄ H ₁₃ N ₃ O ₂	C ₁₄ H ₁₃ N ₃ O ₂
Formula weight	255.27	255.27
Crystal system	Triclinic	Triclinic
Space group	<i>P</i> – 1	<i>P</i> – 1
Unit dimensions		
<i>a</i> (Å)	6.1163(7)	7.9840(9)
<i>b</i> (Å)	7.1376(7)	8.7710(10)
<i>c</i> (Å)	15.2298(11)	9.1420(11)
α (°)	95.414(7)	81.712(8)
β (°)	100.341(8)	73.453(8)
γ (°)	111.084(10)	82.701(9)
Volume (Å ³)	601.06(10)	604.77(12)
<i>Z</i>	2	2
Calculated density (g cm ⁻³)	1.41	1.40
<i>F</i> (000)	268	268
Absorption coefficient (mm ⁻¹)	0.097	0.097
θ range for data collection (°)	3.11–25.00	3.40–27.00
Limits of <i>hkl</i>	–7 ≤ <i>h</i> ≤ 7 –8 ≤ <i>k</i> ≤ 7 –13 ≤ <i>l</i> ≤ 18	–10 ≤ <i>h</i> ≤ 10 –11 ≤ <i>k</i> ≤ 11 –11 ≤ <i>l</i> ≤ 11
Reflections: collected	3085	14,735
Unique (<i>R</i> _{int})	2084 (0.014)	2632 (0.018)
For <i>I</i> > 2 σ (<i>I</i>)	1226	2236
<i>R</i> (<i>F</i>), <i>wR</i> (<i>F</i> ²) for reflections with <i>I</i> > 2 σ (<i>I</i>)	0.050, 0.135	0.046, 0.133
<i>R</i> (<i>F</i>), <i>wR</i> (<i>F</i> ²) for all reflections	0.085, 0.143	0.052, 0.138
Goodness-of-fit on <i>F</i> ²	1.017	1.055
Max/min $\Delta\rho$ (e Å ⁻³) in final ΔF map	0.23/–0.22	0.19/–0.28

Singlet and triplet states: theoretical approach

We employ the quantum-chemical calculations to determine the lowest energy singlet–singlet electronic transitions ($S_0 \rightarrow S_1$) as well as spin-forbidden $S_0 \rightarrow T_1$ transitions from the optimized ground state geometry, whereas $T_1 \rightarrow T_1$ excitation energies and transition intensities were determined for the optimized geometry of the lowest triplet state (T_1), using the unrestricted method suitable for open shell systems. We compare theoretical data obtained at the TD-DFT rB3LYP/6-31 + G(d) methods with experimental singlet–singlet absorption spectra. Theoretically predicted values requiring a shift towards the red for about 600–1000 cm⁻¹ to reproduce experimental spectra.

Fig. 5 shows the predicted lowest-energy singlet–singlet transitions of 138Me-5DAll (A) and 139Me-5DAll (B) together with experimental spectra of absorption in 1,4-dioxane. The lowest calculated energies of singlet–singlet transitions for both compounds were included in Table 5 whereas the lowest predicted energies of singlet–triplet transitions were presented in Table 6.

According to data presented in Fig. 5 and Table 5, the calculated lowest-energy transitions $S_0 \rightarrow S_1$ are of pure $\pi \rightarrow \pi^*$ character at approximately 29,300 cm⁻¹ for 138Me-5DAll and 28,500 cm⁻¹ for 139Me-5DAll.

The observed lowest-energy absorption bands for 138Me-5DAll and 139Me-5DAll can be attributed to the $\pi \rightarrow \pi^*$ transitions and

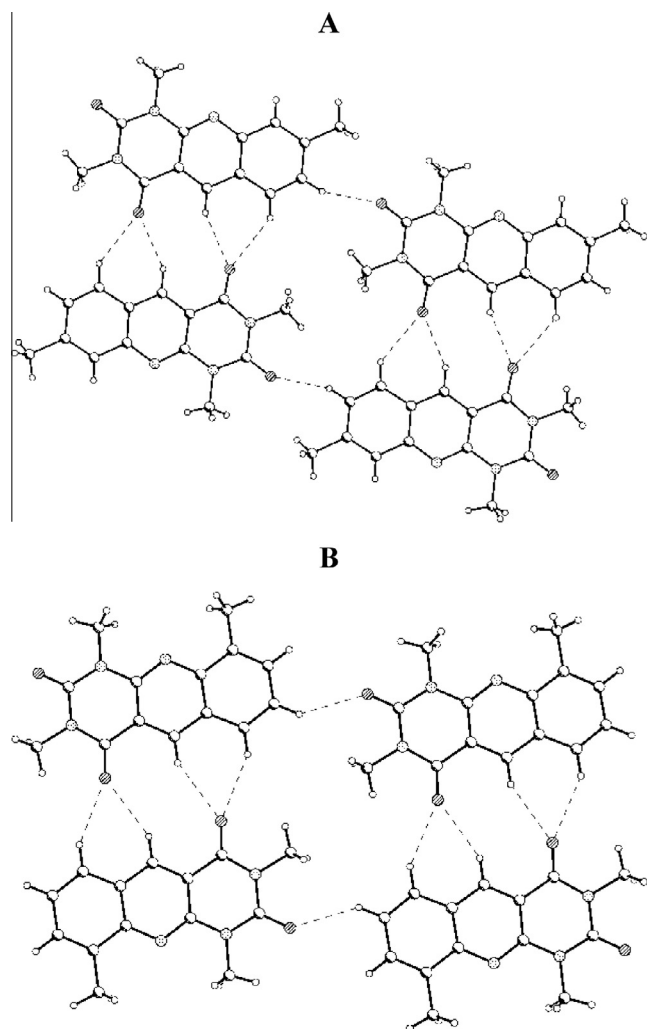


Fig. 4. Hydrogen-bonded molecular tape in the crystal structures of 138Me-5DAll (A) and 139Me-5DAll (B). Hydrogen bonds are depicted by dashed lines.

Table 4
Hydrogen bonds with their lengths (in Å) and angles (in °). Numbering of atoms agree with Fig. 3.

D	H	A	D–H	H···A	D···A	D–H···A
<i>138Me-5DAll</i>						
C-5	H-5	O-4	0.96(2)	2.40(2)	3.286(3)	153.2(15)
C-6	H-6	O-4	0.95(2)	2.59(2)	3.363(3)	139.2(18)
C-7	H-7	O2	0.96(2)	2.36(2)	3.275(3)	159.0(18)
<i>139Me-5DAll</i>						
C-5	H-5	O-4	0.962(16)	2.580(16)	3.4653(15)	151.4(12)
C-6	H-6	O-4	0.979(16)	2.580(16)	3.4499(17)	148.1(12)
C-7	H-7	O-2	0.970(18)	2.524(18)	3.3316(16)	140.7(14)

compared to maxima of absorption spectra registered in 1,4-dioxan, see Fig. 5.

It is noteworthy, that the lowest-energy transitions for 1,3,8-trimethylalloxazine and 1,3,9-trimethylalloxazine, the two compounds which are analogues of investigated in this study compounds, have π, π^* character, accompanied with closely located n, π^* transitions [24]. In consequence, 138Me-5DAll and 139Me-5DAll have higher values of fluorescence quantum yields than their “aza” analogues. The $S_0 \rightarrow S_2$ transitions for both investigated compounds have dominant π, π^* character (Table 5), but they are

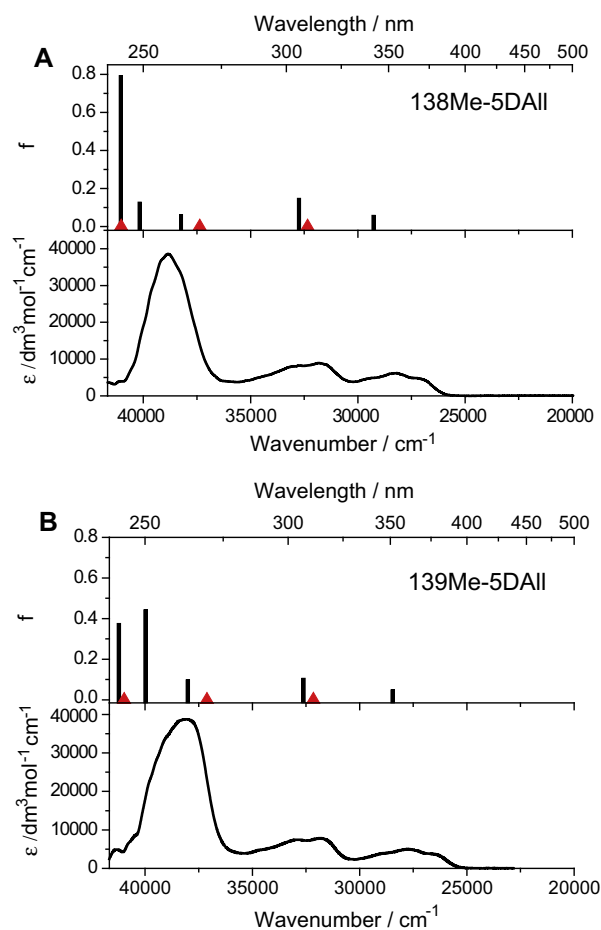


Fig. 5. A – Absorption spectra of 138Me-5DAll; B – Absorption spectra of 139Me-5DAll, both 1,4-dioxan. Predicted transition energies and oscillator strengths f are indicated by solid vertical lines. The (prohibited) transitions involving the n, π^* singlet states are marked by red triangles. (For interpretation of the references to colour in this figure legend, the reader is referred to the web version of this article.)

Table 5

The lowest predicted [rB3LYP/6-31 + G(d)] singlet excitation energies for isolated molecule, starting from the ground state of 138Me-5DAll and 139Me-5DAll with the corresponding oscillator strengths, f .

$S_0 \rightarrow S_i$	138Me-5DAll		139Me-5DAll	
	$E \times 10^{-3} / \text{cm}^{-1}$	f	$E \times 10^{-3} / \text{cm}^{-1}$	f
$\rightarrow S_1$	29.3	0.0590	28.5	0.0487
$\rightarrow S_2$	32.3 ^a	0.0004	32.2 ^a	0.0003
$\rightarrow S_3$	32.7	0.1485	32.6	0.1063
$\rightarrow S_4$	37.4 ^a	0.0001	37.1 ^a	0.0001
$\rightarrow S_5$	38.2	0.0626	38.0	0.0982
$\rightarrow S_6$	40.2	0.1287	39.9	0.4431
$\rightarrow S_7$	41.0 ^a	0	41.0 ^a	0
$\rightarrow S_8$	41.1	0.7931	41.2	0.3759
$\rightarrow S_9$	41.9 ^a	0	41.8 ^a	0
$\rightarrow S_{10}$	43.8	0.4323	43.9	0.3838

^a n, π^* transition, otherwise π, π^* .

accompanied with n, π^* transitions. The energy gap between the two lowest singlet excited states is $|E_{\pi, \pi^*} - E_{n, \pi^*}| = 3400 \text{ cm}^{-1}$ for 138Me-5DAll. The energy separation of the two first singlet states for 139Me-5DAll is $|E_{\pi, \pi^*} - E_{n, \pi^*}| = 4100 \text{ cm}^{-1}$.

Fig. 6 depicts the shape of the highest occupied molecular orbitals (HOMO) and the lowest unoccupied molecular orbitals (LUMO), involved in the transitions to the low-lying excited states

Table 6

The lowest predicted [rB3LYP/6-31 + G(d)] $S_0 \rightarrow T_i$ excitation energies of 138Me-5DAll and 139Me-5DAll with their corresponding oscillator strengths, f .

$S_0 \rightarrow T_i$	138Me-5DAll		139Me-5DAll	
	$E \times 10^{-3}/\text{cm}^{-1}$	f	$E \times 10^{-3}/\text{cm}^{-1}$	f
$\rightarrow T_1$	21.9	0	20.9	0
$\rightarrow T_2$	25.1	0	25.4	0
$\rightarrow T_3$	30.2	0	30.0	0
$\rightarrow T_4$	30.7	0	30.2	0
$\rightarrow T_5$	33.2	0	32.9	0

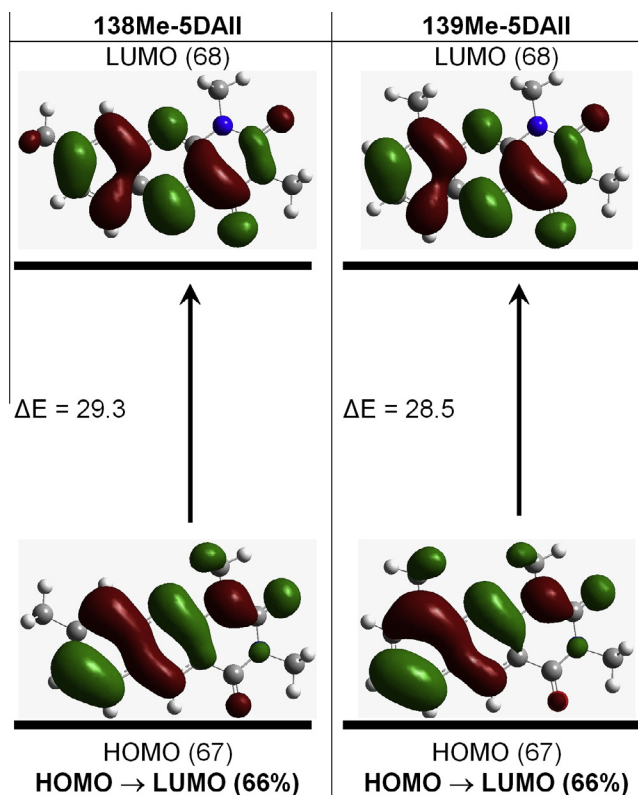


Fig. 6. The shape of the highest occupied molecular orbitals (HOMO) and the lowest unoccupied molecular orbitals (LUMO) for 138Me-5DAll and 139Me-5DAll mainly involved in the lowest singlet–singlet transitions. The isosurfaces correspond to the wave function value of ± 0.02 .

of 138Me-5DAll and 139Me-5DAll. We found that the $S_0 \rightarrow S_1$ transitions of both compounds have dominant contributions (66%) from the HOMO \rightarrow LUMO excitations and are assigned as allowed π, π^* transitions.

In **Table 7** we present results from the triplet state calculations; the lowest $T_1 \rightarrow T_i$ excitation energies and oscillator strengths for 138Me-5DAll and 139Me-5DAll. The lowest excited triplet states has the π, π^* character in both compounds. The predicted UV/Vis transitions for 138Me-5DAll are located at 31,400, 25,800, 22,700, and 18,300 cm^{-1} . For 139Me-5DAll, these transitions are situated at 31,900, 25,600, 22,800, and 19,000 cm^{-1} .

Table 8 collects the calculated bond lengths and dipole moments in the S_0 , S_1 and T_1 states for 138Me-5DAll and 139Me-5DAll. Both compounds studied are planar in all the ground, first excited singlet, and in the triplet states. The compounds are relatively rigid, and the structural changes upon excitation are relatively small. 139Me-5DAll has practically the same dipole moments in its S_0 and S_1 states ($\mu = 3.5$ D and 3.3 D, respectively), similar situation is for 138Me-5DAll ($\mu = 4.2$ D and 4.1 D, respectively), however 138Me-5DAll is more polar than 139Me-5DAll,

Table 7

The lowest predicted [uB3LYP/6-31 + G(d)] $T_1 \rightarrow T_i$ excitation energies of 138Me-5DAll and 139Me-5DAll with their corresponding oscillator strengths, f . (The detectable, theoretically predicted transitions are marked as bold numbers).

$T_1 \rightarrow T_i$	138Me-5DAll		139Me-5DAll	
	$E \times 10^{-3}/\text{cm}^{-1}$	f	$E \times 10^{-3}/\text{cm}^{-1}$	f
$\rightarrow T_2$	6.9	0.0038	7.3	0.0069
$\rightarrow T_3$	11.6	0.0001	11.4	0.0001
$\rightarrow T_4$	12.9	0.0066	12.8	0.0045
$\rightarrow T_5$	15.6	0.0049	15.1	0.0015
$\rightarrow T_6$	16.3	0.0019	15.9	0.0022
$\rightarrow T_7$	16.4	0.0001	16.1	0.0007
$\rightarrow T_8$	18.3	0.0133	19.1	0.0249
$\rightarrow T_9$	21.1	0	20.7	0
$\rightarrow T_{10}$	22.7	0.2064	22.8	0.1994
$\rightarrow T_{11}$	25.8	0.0184	25.6	0.0208
$\rightarrow T_{12}$	26.7	0.0004	26.9	0
$\rightarrow T_{13}$	29.2	0.0004	29.3	0.0008
$\rightarrow T_{14}$	29.7	0.0034	29.8	0.0045
$\rightarrow T_{15}$	29.9	0.0004	30.7	0
$\rightarrow T_{16}$	31.4	0.3127	31.9	0.2781

Table 8

Bond lengths (in Å) and dipole moment in S_0 , S_1 and T_1 states for 138Me-5DAll and 139Me-5DAll.

Bond	138Me-5DAll			139Me-5DAll		
	S_0 ($\mu = 4.2$ D)	S_1 ($\mu = 4.1$ D)	T_1 ($\mu = 5.9$ D)	S_0 ($\mu = 3.5$ D)	S_1 ($\mu = 3.3$ D)	T_1 ($\mu = 5.8$ D)
N10–C10A	1.32	1.34	1.37	1.32	1.34	1.37
C10A–C4A	1.43	1.43	1.39	1.44	1.43	1.39
C4A–C5	1.38	1.41	1.43	1.38	1.41	1.43
N1–C10A	1.39	1.37	1.38	1.39	1.37	1.38
N1–C11	1.47	1.47	1.47	1.47	1.47	1.47
N1–C2	1.39	1.44	1.40	1.39	1.43	1.40
C2–O2	1.22	1.23	1.23	1.22	1.24	1.23
N3–C2	1.40	1.36	1.39	1.40	1.36	1.39
N3–C31	1.47	1.47	1.47	1.47	1.47	1.47
N3–C4	1.40	1.44	1.41	1.40	1.44	1.42
C4–O4	1.23	1.24	1.23	1.23	1.24	1.23
C4–C4A	1.47	1.43	1.45	1.47	1.44	1.45

both in the ground and first excited singlet states. Dipole moments in triplet states (T_1) of both compounds are higher than in the other states ($\mu = 5.9$ D for 138Me-5DAll and 5.8 D for 139Me-5DAll).

Table 9 collects the atomic charges of neutral forms of 138Me-5DAll and 139Me-5DAll in the ground (S_0) and in the first excited singlet state (S_1) in the gas phase, determined by the NBO population analysis. Centres with partial negative charges include nitrogen atoms: N1, N3 and N10, oxygen atoms (O2 and O4) both in S_0 and S_1 states (see also **Fig. 3**, for atom's number). For both compounds, the atoms with the largest positive charge are the carbonyl atoms (C2 and C4), however the charges are larger at C2 than at C4, and these charges do not change much in first excited singlet state. Interestingly, we found some changes between electron density at nitrogen atoms in the ground and in the first excited singlet states. This trend is the same for both compounds, namely the magnitude of the negative charges at nitrogen atoms decrease as follows: $N3 > N10 \approx N1$ in the ground state and $N3 \approx N10 > N1$ in the excited state (see also **Table 9**). Additionally the largest changes in nitrogen atoms charges upon excitation occur at N10 nitrogen atoms and these changes are similar in value for both, 138Me-5DAll and 139Me-5DAll. In our previous work, we found that for 8-methyl-5-deazaalloxazine and 9-methyl-5-deazaalloxazine, the magnitudes of the negative charge at nitrogen atoms in the ground state are as follows, from lower to higher: $N(3) > N(1) > N(10)$ [18]. As we found previously, that the largest growth of the negative charge at heteroatoms of 8-methyl-5-deazaalloxazine and 9-methyl-5-deazaalloxazine upon excitation occurs also on the N10 nitrogen atom of [18].

Table 9
Atomic charges of neutral form of 138Me-5DAll and 139Me-5DAll in the ground (S_0) and in the first excited singlet state (S_1) in the gas phase determined by the NBO population analysis.

Atom	138Me-5DAll		139Me-5DAll		Atom	138Me-5DAll		139Me-5DAll	
	S_0	S_1	S_0	S_1		S_0	S_1	S_0	S_1
C2	0.853	0.851	0.853	0.852	C91	–	–	–0.739	–0.743
C4	0.688	0.684	0.699	0.694	C9A	0.199	0.202	0.191	0.192
C4A	–0.234	–0.249	–0.226	–0.242	C10A	0.452	0.456	0.440	0.443
C5	–0.082	–0.061	–0.091	–0.068	C11	–0.516	–0.516	–0.515	–0.515
C5A	–0.134	–0.149	–0.120	–0.135	C31	–0.519	–0.518	–0.519	–0.520
C6	–0.202	–0.195	–0.217	–0.211	N10	–0.488	–0.499	–0.486	–0.496
C7	–0.252	–0.257	–0.252	–0.257	N1	–0.481	–0.476	–0.478	–0.476
C8	–0.013	–0.014	–0.229	–0.229	N3	–0.511	–0.508	–0.513	–0.509
C9	–0.245	–0.243	–0.021	–0.016	O2	–0.630	–0.631	–0.629	–0.631
C81	–0.743	–0.745	–	–	O4	–0.606	–0.596	–0.606	–0.597

Conclusions

We described spectral and photophysical properties of two trimethyl- derivatives of 5-deazaalloxazine using both experimental and theoretical methods and compared them to those of their alloxazine analogues. We conclude that although 5-deazaalloxazines and alloxazines have similar structures, some differences in their spectroscopy and photophysics are noted. The spectra of 138Me-5DAll and 139Me-5DAll, generally show a blue shift in absorption and fluorescence maxima in comparison to their “aza” analogues.

Additionally, we found that solvent effects have small influence on absorption and emission maxima of investigated compounds, however solvents affects their fluorescence quantum yields and fluorescence lifetimes. The values of fluorescence quantum yields are higher and fluorescence lifetimes are longer in alcohols as compared to those in aprotic solvents. According to theoretical calculations using TD-DFT methods for isolated molecules, we can state that the lowest-energy transitions have π, π^* character, being unaccompanied by the closely-located n, π^* transitions, as is the case for derivative of alloxazine. Also lowest triplet excited states of 138Me-5DAll and 139Me-5DAll have π, π^* character. On the basis of theoretical calculations, we can also state, that the biggest change in electron density, during $S_0 \rightarrow S_1$ transition, occurs at nitrogen atom N(10), if we consider only the heteroatoms.

We described also the crystal structures of 138Me-5DAll and 139Me-5DAll, determined by X-ray diffraction methods. The crystal structures of investigated compounds are similar, belonging to the same space group and the molecules in these crystals are connected by similar systems of hydrogen bonds.

Acknowledgments

This study was supported by the research grant DEC-2012/05/B/ST4/01207 from The National Science Centre of Poland (NCN). All of the calculations were performed at the PL-Grid project and by the Poznań Supercomputing and Networking Centre.

References

- [1] L.V. Bystrykh, N.I. Govorukhina, L. Dijkhuizen, J.A. Duine, *Eur. J. Biochem.* 247 (1997) 280.
- [2] D. Vargo, A. Pokora, S.-W. Wang, M.S. Johns, *J. Biol. Chem.* 256 (1981) 6027.
- [3] P. Hemmerich, V. Massey, H. Fenner, *FEBS Lett.* 84 (1977) 21. and references cited therein.
- [4] A. Koziółowa, N.V. Visser, J. Koziół, M.M. Szafran, *J. Photochem. Photobiol. A* 93 (1996) 157.
- [5] T. Kawamoto, Y. Ikeuchi, J. Hiraki, Y. Eikyu, K. Shimizu, M. Tomishima, K. Bessho, F. Yoneda, Y. Mikata, M. Nishida, K. Ikehara, T. Sasaki, *Bioorg. Med. Chem. Lett.* 5 (1995) 2109.

- [6] Y. Ikeuchi, M. Sumiya, T. Kawamoto, N. Akimoto, Y. Mikata, M. Kishigami, S. Yano, T. Sasaki, F. Yoneda, *Bioorg. Med. Chem.* 8 (2000) 2027.
- [7] Y. Kanaoka, Y. Ikeuchi, T. Kawamoto, K. Bessho, N. Akimoto, Y. Mikata, M. Nishida, S. Yano, T. Sasaki, F. Yoneda, *Bioorg. Med. Chem.* 6 (1998) 301.
- [8] J.M. Wilson, G. Henderson, F. Black, A. Sutherland, R.L. Ludwig, K.H. Vousden, D.J. Robins, *Bioorg. Med. Chem.* 15 (2007) 77.
- [9] H.I. Ali, N. Ashida, T. Nagamatsu, *Bioorg. Med. Chem.* 16 (2008) 922.
- [10] J.H. Burckhalter, F.H. Tendick, E.M. Jones, P.A. Jones, W.F. Holcomb, A.L. Rawlins, *J. Am. Chem. Soc.* 70 (1948) 1363.
- [11] H.I. Ali, N. Ashida, K.S. Won, Y.M. Kwang, *Bioorg. Med. Chem. Lett.* 3 (1993) 2631.
- [12] J. Joule, G. Smith, *Heterocyclic Chemistry*, ELBS Low Price Edition, London, 1979, p. 126.
- [13] S. Dudkin, V.O. Iaroshenko, V.Ya. Sosnovskikh, A.A. Tolmachev, A. Villingner, P. Langer, *Org. Biomol. Chem.* 11 (2013) 5351.
- [14] Z. Wang, C. Rizzo, *J. Org. Lett.* 2 (2000) 227.
- [15] S. Dudkin, PhD thesis, Rostock, January 2013, Design and Synthesis of Pyrimidine C-Nucleosides, 5-Polyfluoroalkyl-5-deazaalloxazines and Spiro[pyrimido[4,5-b]quinoline-3',5'-indoline-2'-one]-3,10-dihydro-2,4-diones.
- [16] A. Koziółowa, N.V. Visser, J. Koziół, M.M.M. Szafran, *J. Photochem. Photobiol. A* 93 (1996) 157.
- [17] S. Salzmann, V. Martinez-Junza, B. Zorn, S.E. Braslavsky, M. Mansurova, C.M. Marian, W. Gärtner, *J. Phys. Chem. A* 113 (2009) 9365.
- [18] D. Prukata, M. Taczowska, M. Gierszewski, T. Pędziński, M. Sikorski, *J. Fluoresc.* 24 (2014) 505.
- [19] E. Sikorska, I.V. Khmelinskii, W. Prukata, S.L. Williams, M. Patel, D.R. Worrall, J.L. Bourdelande, J. Koput, M. Sikorski, *J. Mol. Struct.* 689 (2004) 121.
- [20] E. Sikorska, I.V. Khmelinskii, W. Prukata, S.L. Williams, M. Patel, D.R. Worrall, J.L. Bourdelande, J. Koput, M. Sikorski, *J. Phys. Chem. A* 108 (2004) 1501.
- [21] M. Sikorski, D. Prukata, M. Insińska-Rak, I. Khmelinskii, D.R. Worrall, S.L. Williams, J. Hernando, J.L. Bourdelande, J. Koput, E. Sikorska, *J. Photochem. Photobiol. A* 200 (2008) 148.
- [22] S. Salzmann, Ch.M. Marian, *Photochem. Photobiol. Sci.* 8 (2009) 1655.
- [23] E. Sikorska, I.V. Khmelinskii, J.L. Bourdelande, A. Bednarek, S.L. Williams, M. Patel, D.R. Worrall, J. Koput, M. Sikorski, *Chem. Phys.* 301 (2004) 95.
- [24] M. Bruszyńska, E. Sikorska, A. Komasa, I. Khmelinskii, L.F.V. Ferreira, J. Hernando, J. Karolczak, M. Kubicki, J.L. Bourdelande, M. Sikorska, *Chem. Phys.* 361 (2009) 83.
- [25] F. Yoneda, Y. Sakuma, *J. Chem. Soc., Chem. Commun.* 6 (1976) 2003.
- [26] F. Yoneda, Y. Sakuma, S. Mizumoto, R. Ito, *J. Chem. Soc., Perkin Trans. 1* (1976) 1805.
- [27] H. Goldner, G. Dietz, E. Carstens, *Liebigs Ann. Chem.* 694 (1966) 142.
- [28] ACD/ChemSketch; version 4.55, Advanced Chemistry, Development Inc., Toronto, Canada, Ed., 2000.
- [29] Agilent Technologies, CrysAlis PRO (Version 1.171.33.36d), Agilent Technologies, 2010.
- [30] L.J. Farrugia, *J. Appl. Cryst.* 30 (1997) 565.
- [31] A. Altomare, G. Cascarano, C. Giacovazzo, A. Guagliardi, *J. Appl. Cryst.* 26 (1993) 343.
- [32] A.D. Becke, *J. Chem. Phys.* 98 (1993) 5648.
- [33] R. Ditchfield, W.J. Herre, J.A. Pople, *J. Chem. Phys.* 54 (1971) 724.
- [34] M.J. Frisch, G.W. Trucks, H.B. Schlegel, G.E. Scuseria, M.A. Robb, J.R. Cheeseman, V.G. Zakrzewski, A.J. Jr. Montgomery, R.E. Stratmann, J.C. Burant, S. Dapprich, J.M. Millam, A.D. Daniels, K.N. Kudin, M.C. Strain, O. Farkas, J. Tomasi, V. Barone, M. Cossi, R. Cammi, B. Mennucci, C. Pomelli, C. Adamo, S. Clifford, J. Ochterski, G.A. Petersson, P.Y. Ayala, Q. Cui, K. Morokuma, D.K. Malick, A.D. Rabuck, K. Raghavachari, J.B. Foresman, J. Cioslowski, J.V. Ortiz, B.B. Stefanov, G. Liu, A. Liashenko, P. Piskorz, I. Komaromi, R. Gomperts, R.L. Martin, D.J. Fox, T. Keith, M.A. Al-Laham, C.Y. Peng, A. Nanayakkara, C. Gonzalez, M. Challacombe, P.M.W. Gill, B. Johnson, W. Chen, M.W. Wong, J.L. Andres, C. Gonzalez, M. Head-Gordon, E.S. Replogle, J.A. Pople, GAUSSIAN 03, Revision B05, Gaussian Inc, Wallingford, CT., 2003.